Journal

Rapid Oxidation Characterization of Ultra-High Temperature Ceramics

Sigrun N. Karlsdottir[†] and John W. Halloran

Materials Science and Engineering Department, University of Michigan, Ann Arbor, Michigan 48109-2136

Here, a novel method for testing ultra-high-temperature ceramics (UHTC) at a high temperature, rapidly, at a low cost is introduced. A self-supported, self-heated ribbon specimen is used with a table-top apparatus to achieve the necessary high temperatures. This method enables a large temperature–time–composition parameter space to be covered by rapidly producing a large set of postoxidation samples for analysis. The complex oxide scale known to form during oxidation of UHTC materials is shown to be easily reproduced using this method. A ZrB_2–SiC (15 vol%) UHTC material was tested at 1700°C for 15 min. The oxide scale consists of a thin outermost silica (SiO_2) layer and a zirconia (ZrO_2) columnar layer with small amounts of SiO_2 embedded between the ZrO_2 columns. A region of SiC-depleted zone was observed between the unreacted core and the ZrO_2 layer. The measured thickness of the oxide scale was 102 μm and ∼ 120 μm for the SiC-depleted zone.

I. Introduction

RECENTLY, interest in ultra-high temperature ceramics (UHTC) has increased significantly due to the drive to produce a reusable thermal protection system and other components for future generations of hypersonic aerospace vehicles.[1] Most modern designs of hypersonic vehicles incorporate sharp aero-surfaces to increase aerodynamic performance. These designs require materials capable of operating in an extreme re-entering environment, such as an oxidizing atmosphere at temperatures above 1700°C and corrosive gases at high velocities.[2] Today, there are few fully developed materials that meet the needs of thermal protection systems for sharp aero-surfaces and so UHTC are receiving more attention as the solution.

UHTC are a class of refractory materials including transition metal borides, carbides, and nitrides. The refractory borides, i.e. ZrB_2 and HfB_2, have extremely high melting temperatures, >3000°C, high thermal conductivity, high hardness, and retained strength and chemical stability at elevated temperatures.[3] As early as 1953, ZrB_2- and HfB_2-based composites were identified by Hoffman,[4] followed by groups led by Berkowitz-Mattuck[5] and Kaufman *et al.*,[6] as the most promising material for hypersonic applications. In the 1970s, Kaufman *et al.*[7,8] showed that by addition of SiC to ZrB_2 and HfB_2, the oxidation resistance could be greatly improved. Tripp[9] and Tripp and Graham[10] confirmed Kaufman's results and provided additional information such as microstructural studies of the oxide scale. Past studies by Levine *et al.*,[11] Nguyen *et al.*,[12] Opila *et al.*,[13] Monteverde *et al.*,[14–18] Scatteia *et al.*,[19] Monteverde and Bellosi,[20] Fahrenholtz Hilmas and colleagues,[21,22] and others[23,24] have also shown that addition of SiC to ZrB_2 and HfB_2 increases densification, thermal shock, and oxidation resistance of the

composites. These researchers have discovered that ZrB_2–SiC and HfB_2–SiC composites form a complex oxide scale after oxidation at elevated temperatures. The oxide scale is composed of refractory oxide skeleton and amorphous glass components that provide oxidation resistance of the composites at high temperatures.

Despite the fact that it has been almost 50 years since researchers started to explore UHTC materials the oxidation mechanisms of these materials are still not well understood. This is primarily due to the complexity of the oxide scale and limited information. Also, much of the oxidation experiments that have been conducted were at temperatures below 1700°C. The main exception is NASA's Arc Jet Facility used to simulate aerodynamic heating. It is capable of reaching temperatures from 1700° to 2500°C.[1,21,25,13] Arc jet testing is expensive due to the high power used during testing (40–75 MW), and the facilities are operated primarily to support the government aerospace research and developmental testing.[25] Nongovernmental groups can apply for its use, but it is both time consuming and complicated.[26]

Here, we report a novel method for testing UHTC materials at high temperatures rapidly at low cost. A self-supported, self-heated ribbon specimen is used with a table-top apparatus to achieve the necessary high temperatures for UHTC oxidation experiments. The present work introduces the design of the system and function. Also, the complex oxide scale that forms during oxidation of UHTC is shown here to be easily reproduced using the ribbon method.

II. The Ribbon Method

(1) The Self-Supported Ribbon Specimen

The design of the table-top apparatus is based on the fact that the UHTC materials are metallic conductors. A miniaturized self-supportive UHTC specimen is resistively heated by passing a modest current. The specimen is fabricated by reducing the thickness of a matchstick-size sample in the center to make a ribbon with a thickness of 400–500 μm. The ribbon, herein called the hot zone, can reach very high temperatures when the current is passed into the thicker ends of the specimen. The thicker ends of the specimen will remain relatively cool, while the hot zone can reach the desired temperature. With this geometry the specimen is self-supportive (Fig. 1). The hot zone is thus not in contact with foreign material. This is important, because at these high temperatures, the specimen may react with the materials it contacts. The specimen is in open air during testing, and it has a small heat load, and so diagnostics can be brought close to it during oxidation.

(2) The Table-Top Apparatus

A table-top apparatus provides the current and controls the temperature of the specimen. The control unit of the apparatus consists of a control panel (MHI BPAN-O™, Micropyretics Heaters Int., Cincinnati, OH), and a programmable temperature controller (Model 2416, Eurotherm, Leesburg, VA). The power controller is a single-phase silicon (Si)-controlled rectifier (SCR) with an advanced current limit and a soft start feature. A stepdown transformer is a part of the apparatus and is connected to the controller to give the desired secondary current in the
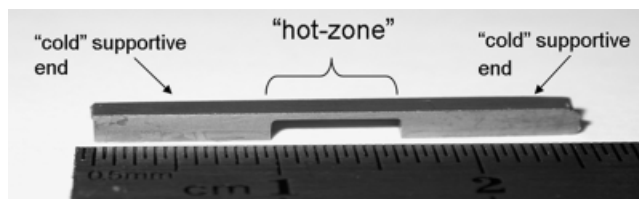
Fig. 1. Digital image of the self-supported, self-heated ribbon specimen.

range of 0–125 A. The power input used to heat the ribbon specimen to temperatures from 900° to 2000°C is around 90–125 W, where the voltage across the specimen is on the order of 1 V and the current ranges from 90 to 125 A.

The temperature sensor of the apparatus is a micro optical infrared pyrometer that can measure temperature from 900° to 3300°C with a fast response time (minimum 1 ms). The micro pyrometer is a single-color pyrometer with a wavelength of 1 μm and a bandwidth of 0.7–1.1 μm. The micro pyrometer is focused on the hot zone of the specimen and provides the temperature signal to the temperature controller. The amount of current passed through the sample is controlled with the power controller to obtain the desired temperature-time schedule. The UHTC specimen can be quickly heated and cooled due to the fast response of the temperature controller and the pyrometer and the size of the miniaturized sample. Any time-temperature profile, cyclic, or static oxidation can be conducted using the pyrometer signal as the control variable. With the table-top apparatus and the ribbon specimen, oxidation experiments at temperatures in the range of 900°–2000°C can be performed, without creating a difficult-to-manage heat load in the surroundings due to the small size of the specimen. A similar approach was used by Cabrera and Kirner[27] for the design of a cyclic metal-oxidation apparatus. Cabrera and Kirner[27] resistively heated thin Si-coated steel foils, 50-μm thick, but these were only capable of reaching temperatures in the range of 400°–1000°C.

Figure 2(a) shows the self-supported miniaturized specimen connected to the table-top apparatus. Figure 2(b) shows the

specimen sitting on a simple (copper) Cu/(silver) Ag bridge fixed with alligator clips, which can serve as voltage probes. The bridge consists of Cu plates that hold up Ag sheets where the thicker ends of the specimen sit. The Cu plates are connected to the current leads and fixed to a thermal insulation base plate (Transite® HT, Monaco, MI). Ag was used for connecting the specimen to the Cu plates due to its high conductivity and oxidation resistance (Cu was not suitable due to its poor oxidation resistance). Thin alumina (Al_2O_3) sheets were used between the alligator clips and the sample as heat shields, to avoid over heating of the alligator clips.

Temperature, current, and voltage are recorded by a LabView DAQ. An AC clamp on adapter is clamped on the secondary wire in the circuit to detect the current going through the specimen, and then transfers it to a data acquisition card (DAQ) (NI USB-6009, National Instruments Corporation, Austin, TX) connected to a computer. The temperature measured with the micro pyrometer is transferred to the computer through a RS-232 cable. To process the data from the DAQ and the RS-232 cable, LabVIEW from National Instruments is used. A LabVIEW program was designed to collect and save the temperature, current, and voltage data sampled during testing. The LabVIEW program samples the signal from the DAQ and the RS-232 cable (connected to the pyrometer) and plots the RMS current versus time and the temperature versus time. The data are collected at a sampling frequency of 4 Hz, i.e. the sampling time is 250 ms. Figure 3 shows an example of a temperature and a current profile of a ribbon specimen tested in the apparatus at 1600°C for 15 min.

III. Experimental Procedure

(1) Material Fabrication

The UHTC material, ZrB_2—15 vol% SiC, used in this work was provided by The Institute of Science and Technology for Ceramics (CNR-ISTEC) in Faenza, Italy. Details of the properties and processing are presented in more detail elsewhere.[28] The fabrication of the self-supporting specimens is performed in two steps. Firstly, the bulk material is cut with a wire-EDM machine
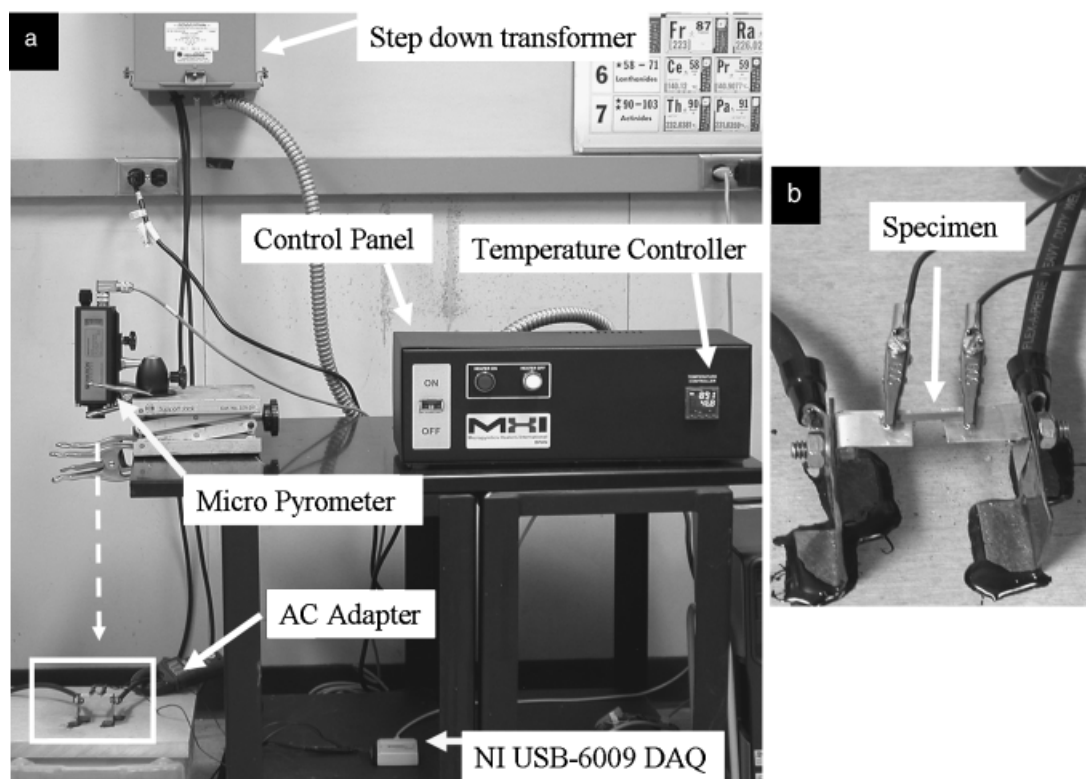

Fig. 2. (a) The self-supported ribbon specimen (white box) and its table-top apparatus, (b) the specimen sitting on a copper (Cu)/silver (Ag) holder (magnification of the white box in the lower left corner of (a)).
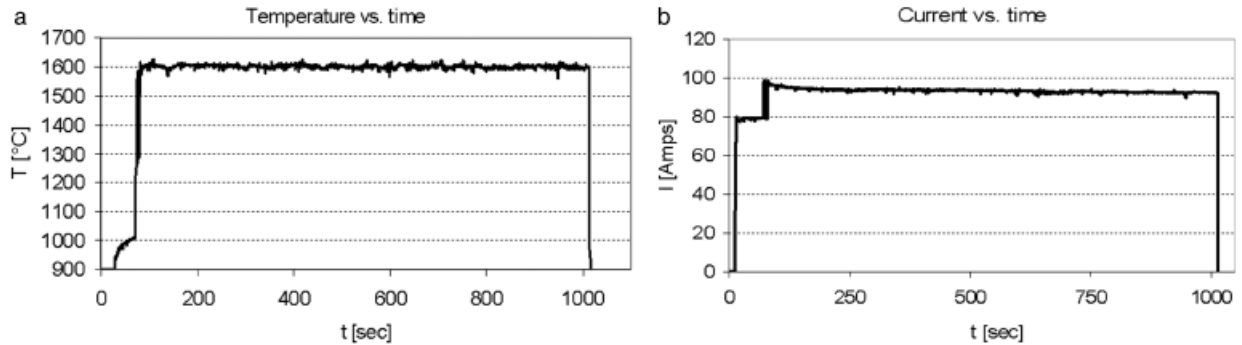
Fig. 3. (a) Temperature profile, (b) and a current profile of a specimen tested at 1600°C for 15 min.

into 2.3 mm × 2.0 mm × 25 mm bars. The bars are then reduced in thickness in the center with a mechanical grinder (220 grit—diamond wheel) to make the thin ribbon hot zones, with a thickness of 400–500 μm; see Fig. 1.

(2) Oxidation Testing

To verify whether the ribbon specimen method could reproduce the complex oxide scales that form during high-temperature experiments on UHTC, ZrB$_2$–SiC specimens (CNR-ISTEC, Italy) were tested in the high-temperature apparatus. The specimen was tested at 1700°C in stagnant ambient air for 15 min, at a heating rate of 480°C/min and free cooling (767°C/s). The fast cooling rate is due to the fast thermal response time (2.98 ms at 1700°C) of the specimen, which is dependent on the thickness of the specimen ($t = 420$ μm) and its thermal diffusivity ($1.41 × 10^{-5}$ m^2/s at 1700°C). The fast heating minimizes the oxidation before the isothermal run at 1700°C.

The tested specimen was stored in moisture-free desiccators. A cross section of the oxidized specimen was prepared for microstructural analysis by nonaqueous polishing procedures down to a 1 μm finish. The composition and morphology of the multilayer oxide scale formed after the oxidation test were characterized by scanning electron microscopy (SEM; Philips XL30, Hillsboro, OR), backscattering electron microscopy (BSE; Philips), X-ray energy dispersive spectroscopy (XEDS; UTW Si–Li Solid State X-ray Detector with integrated EDAX Phoenix XEDS system, Mahwah, NJ), and electron microprobe analyzer (EPMA; Cameca SX100 Microprobe, Gennevilliers, France). Analyses were performed on the surface of the specimen and cross section.

IV. Results and Discussion

When monolithic ZrB$_2$(s) oxidizes an oxide scale composed of zirconia, ZrO$_2$(s), and boron oxide liquid, B$_2$O$_3$(l), forms by the reaction[16]

$$ZrB_2(s) + 5/2O_2(g) \rightarrow ZrO_2(s) + B_2O_3(l) \quad (1)$$
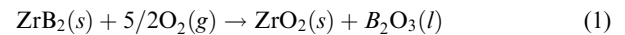
The liquid B$_2$O$_3$ forms a continuous passive layer acting as a barrier to oxygen (O) diffusion, which results in passive oxidation of ZrB$_2$ and a parabolic oxidation kinetics below ca. 1000°C. Above 1000°C, the oxidation resistance of ZrB$_2$ is poor due to volatilization of B$_2$O$_3$.[21] The kinetics is then controlled by the competition between mass gain (ZrO$_2$(s) and B$_2$O$_3$(l) formation) and mass loss (B$_2$O$_3$(g) vaporization). At higher temperatures, ZrB$_2$ actively oxidizes due to volatilization of the B$_2$O$_3$ liquid, and results in a porous, nonprotective ZrO$_2$ layer.[5,16,21–23] Researchers have reported that by adding SiC to ZrB$_2$, the oxidation resistance of the composite above 1200°C is improved by the formation of a less volatile silica (SiO$_2$)-rich glass on the exposed surface[1,10,21,11,13,18]:

$$SiC(s) + 3/2O_2(g) \rightarrow SiO_2(s) + CO(g) \quad (2)$$
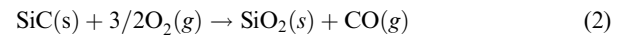
The SiO$_2$-rich layer has been reported to provide passive oxidation resistance to at least 1500°C due to the lower volatility of SiO$_2$ compared with B$_2$O$_3$ at these temperatures.

Figure 4 shows an SEM image of the surface of the tested ZrB$_2$–15 vol% SiC specimen. The bright peaks shown in Fig. 4(a) indicate ZrO$_2$ peaks embedded in a SiO$_2$-rich glass matrix, verified by XEDS analysis (Fig. 4(b)). A BSE image of the cross section of the specimen (Fig. 5) shows that the oxide
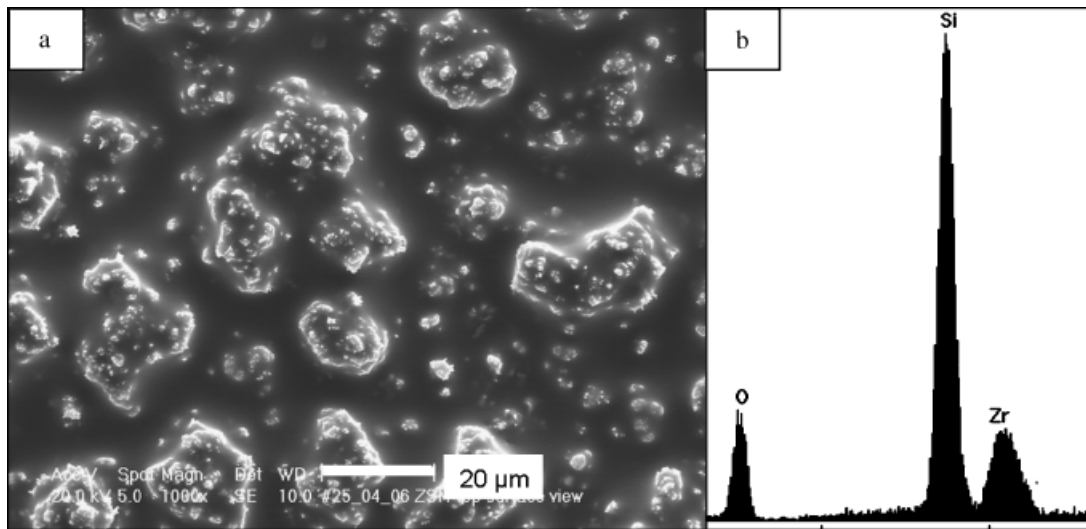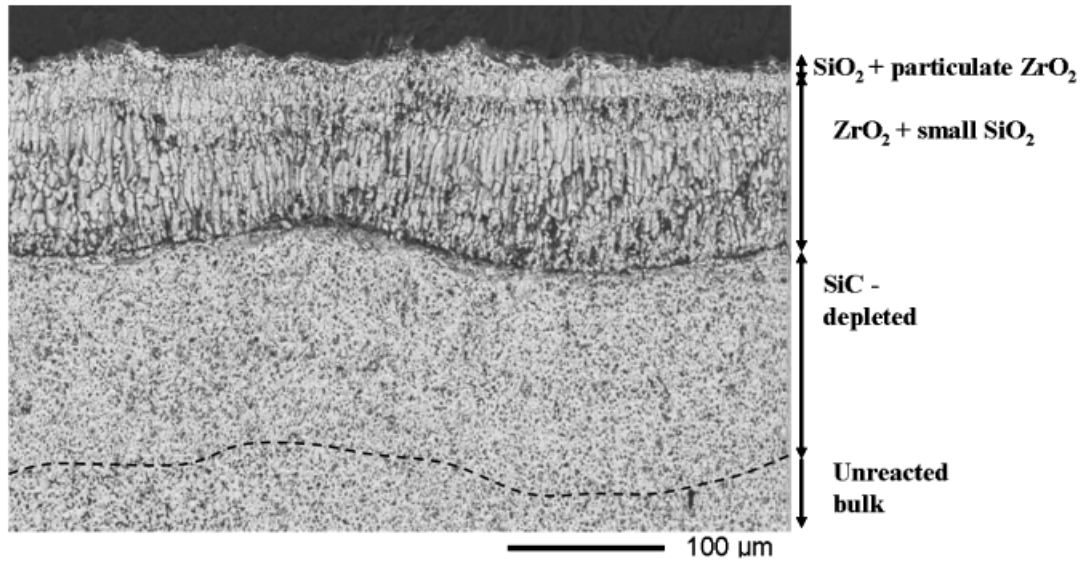

Fig. 4. Surface view of the ZrB$_2$/SiC composite tested at 1700°C for 15 min, (a) zirconia (ZrO$_2$) peaks embedded in a silica (SiO$_2$) glass matrix, (b) X-ray energy dispersive spectroscopy analysis of the surface.

Fig. 5. Image of a cross section of a ZrB_2/SiC composite tested at 1700°C for 15 min. Multilayer oxide scale, consisting of an unaffected substrate, a SiC-depleted zone, a columnar zirconia (ZrO_2) layer, and a thin superficial layer of silica (SiO_2) glass.

scale of the specimen is multilayered and multicomponent. The chemical composition of the oxide scale was characterized by XEDS and EPMA techniques. The oxide scale consists of a thin superficial layer of a SiO_2 glass containing a small amount of particulate ZrO_2; the second layer mainly consists of columnar ZrO_2 grains. The columnar ZrO_2 layer has a small amount of

SiO_2 glass embedded between the ZrO_2 columns. The thickness of the oxide scale was measured to be on average 102 μm. A region of the SiC-depleted zone was observed between the unreacted core and the ZrO_2 layer. The SiC-depleted zone is large ca. 120 μm, which results in a small region of unreacted material (core). This is evident from the elemental maps from the EPMA
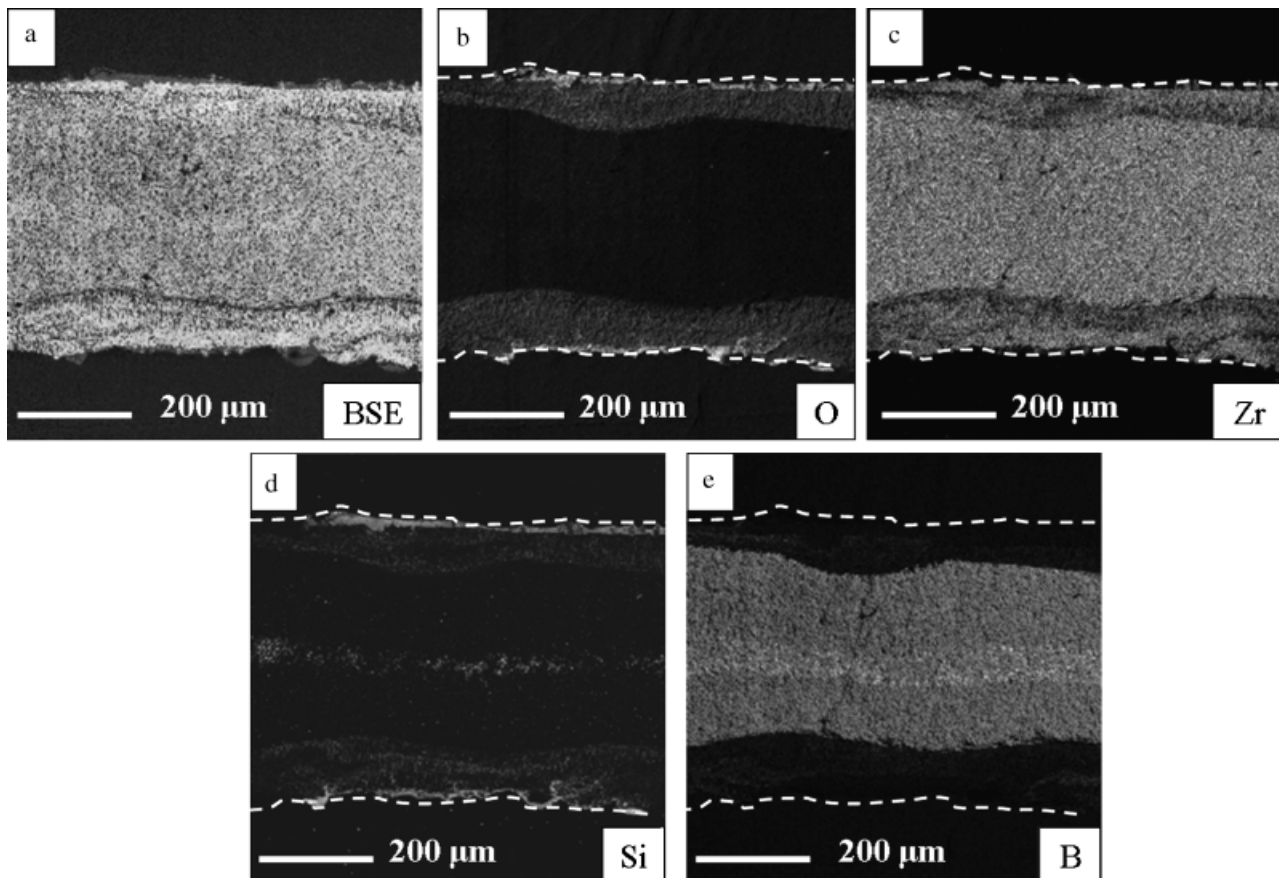
Fig. 6. (a) Backscattering electron microscopy (BSE) image of the cross section of the ZrB_2/SiC specimen tested at 1700°C for 15 min, (b) O map, showing the oxygen distribution in the silica (SiO_2) and zirconia (ZrO_2) scales, (c) Zr map, (d) Si map, showing the large SiC-depleted region and the thin strip of the unreacted core, (e) B map, showing the thickness of the oxide scale and the unreacted ZrB_2 in the SiC-depleted zone. The white dashed line in (b–e) outlines the thickness of the specimen. The white color in the maps indicates the higher intensity of X-rays detected for each element, while the black region represents zero detected intensity of the element.

analysis (Fig. 6). The existence of a SiC-depleted layer in oxidized ZrB_2/HfB_2–SiC composites has been reported by other researchers in the field.[10,17,21,25]

The EPMA analyses were performed on the cross section shown in the BSE image in Fig. 6(a). The analyses were mainly performed to verify the results from the XEDS on the distribution of the elements: Si, O, zirconium (Zr), and boron (B). Also, B could not be detected with the SEM/XEDS machine used; thus, EPMA analyses were performed to give us information on whether there existed any borosilicate glass or B_2O_3 in the oxide scale. B_2O_3 was not detected in the SiO_2-rich scale or in the ZrO_2 columnar region with EPMA; this is likely due to the small amount of B_2O_3 existing in the oxide scale, which could not be detected with the scanning speed (20 ms) used for the EPMA analysis. The small amount of B_2O_3 is expected due to the high temperature (1700°C) that the specimen experienced. B_2O_3 is believed to start volatilizing extensively at temperatures above 1200°C for a monolithic material.[16] Also, the outermost layer, the thin SiO_2-rich scale, will not have the same effective role in limiting O diffusion at 1700°C as at lower temperatures. The use of SiO_2-forming ceramics at high temperatures has been reported to be limited to a maximum of 1725°C because of rapid oxidation, potential volatility, scale melting, and scale/substrate reactions of the SiO_2 formed.[29]

From the O, Zr, and Si maps (Figs. 6(a)–(e)), the small amount of interstitial SiO_2 glass in the ZrO_2 columnar layer can be easily identified. These maps also show clearly the thin outermost SiO_2-rich layer (Figs. 6(b)–(d)). As mentioned above, the SiO_2 scale contains small amounts of particulate ZrO_2. A higher magnification of the SiO_2-rich scale and the particulate ZrO_2 is shown in Fig. 7; small peaks of the particulate ZrO_2 are clearly evident. These peaks were also observed from the surface of the specimen (Fig. 4(a)). The nature of the particulate ZrO_2 peaks and their formation mechanism are discussed elsewhere.[30]

Our results are consistent with the results reported by other researchers in the field. Levine *et al.*[11] found that the oxide scale of a ZrB_2–SiC (20 vol%) composite, tested in air at 1927°C for ten 10-min cycles, was composed of large ZrO_2 grains in a SiO_2-rich glassy phase, where the outermost part of the oxide scale contained less SiO_2 glass than the inner most part of the scale. They also found that after oxidation testing in air at 1627°C for ten 10-min cycles (total 100 min), the oxide scale of the composite was composed of two layers: an outer SiO_2 layer and a ZrO_2+SiO_2 layer. A porous SiC-depleted layer was also observed beneath the oxide scale. Gasch *et al.*[25] performed testing on HfB_2–SiC (20 vol%) composites in a simulated re-entry environment using the NASA Ames Arc Jet Facility. The specimens were tested at 1690°C for two 10-min cycles. Gash *et al.*[25] concluded that, for the two conditions, a passive oxidation of the SiC plays a role in determining the steady-state surface temperature below 1700°C. This is consistent with our results; the
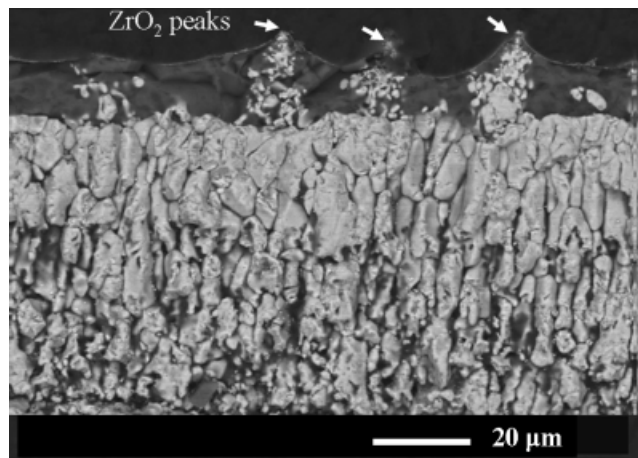
oxide scale of the ZrB_2–SiC (15 vol%) specimen tested at 1700°C for 15 min consisted mainly of a ZrO_2 columnar layer with a small amount of SiO_2 embedded, and a thin outermost SiO_2 layer. The large SiC-depleted zone observed for the specimen indicates that the SiO_2 layer does not provide enough protection for a passive oxidation at 1700°C. This is consistent with the prediction by Jacobson[29] about the limited use of SiO_2-forming ceramics at higher temperatures (maximum 1725°C).

V. Conclusion

The complex oxide scale known to form during oxidation of UHTC is shown to be easily reproduced by using the ribbon specimen method. The oxide scale of a ZrB_2–SiC (15 vol%) specimen tested at 1700°C for 15 min consisted of a thin outermost SiO_2 layer and a ZrO_2 columnar layer with small amounts of SiO_2 embedded between the ZrO_2 columns. A region of SiC-depleted zone was observed between the unreacted core and the ZrO_2 layer. The measured thickness of the oxide scale was 102 μm and the ~120 μm for SiC-depleted zone.

The table-top apparatus with its ribbon specimen enables us to perform oxidation experiments at temperatures above 900°C and as high as 2000°C with power input only around 100 W, without creating a difficult-to-manage heat load in the surroundings due to the small size of the specimen. This new design is a valuable alternative for exposure of UHTC to high temperatures.

References

[1]M. M. Opeka, I. G. Talmy, and J. A. Zaykoski, "Oxidation-Based Materials Selection for 2000°C+Hypersonic Aerosurface: Theoretical Considerations and Historical Experience," *J. Mater. Sci.*, **39** [19] 5887–904 (2004).

[2]P. Kolodziej, "Aerothermal Performance Constraints for Hypervelocity Small Radius Unswept Leading Edges and Nosetips"; NASA Technical Memorandum, 112204, July 1997.

[3]R. Telle, L. S. Sigl, and K. Takagi, "Transition Metal Boride Ceramics"; pp. 803–945 in *Handbook of Ceramic Hard Materials*, Vol. 2, Edited by R. Reidel. Wiley-VCH, Weinheim, Germany, 2000.

[4]C. A. Hoffman, "Preliminary Investigation of Zirconium Boride Caramels for Gas-Turbine Blade Applicatons"; NASA Technical Memorandum E52L15a, Lewis Flight Propulsion Laboratory, Cleveland, OH, 1953.

[5]J. B. Berkowitz-Mattuck, "High-Temperature Oxidation, III. Zirconium and Hafnium Diborides," *J. Electrochem. Soc.*, **113**, 908–14 (1966).

[6]L. Kaufman, E. V. Clougherty, and J. B. Berkowitz-Mattuck, "Oxidation Characteristics of Hafnium and Zirconium Diboride," *Trans. Metall. Soc. AIME*, **239** [4] 458–66 (1967).

[7]L. Kaufman, "Boride Composites–A New Generation of Nose Cap and Leading Edge Materials for Reusable Lifting Reentry Systems," AIAA Advanced Space Transportation Meeting. *Am. Inst. Aeronaut. Astronaut.*, 270–8 (1970).

[8]L. Kaufman and H. Nesor, "Stability Characterization of Refractory Materials under High Velocity Atmospheric Flight Conditions, Part I, Vol. I, Summary"; Technical Report no. AMFL-TR-69-84, Air Force Materials Laboratory, Wright-Patterson Air Base, OH, 1970.

[9]W. C. Tripp and H. C. Graham, "Thermogravimetric Study of Oxidation of ZrB_2 in Temperature Range of 800 Degrees to 1500 Degrees," *J. Electrochem. Soc.*, **118**, 1195–971 (1971).

[10]W. C. Tripp, H. H. Davis, and H. C. Graham, "Effect of SiC Addition on the Oxidation of ZrB_2," *Am. Ceram. Soc. Bull.*, **52** [8] 612–6 (1973).

[11]S. R. Levine, E. J. Opila, M. C. Halbig, J. D. Kiser, M. Singh, and J. A. Salem, "Evaluation of Ultra-High Temperature Ceramics for Aeropropulsion Use," *J. Eur. Ceram. Soc.*, **22**, 2757–67 (2002).

[12]Q. N. Nguyen, E. J. Opila, and R. C. Robinson, "Oxidation of Ultrahigh Temperature Ceramics in Water Vapor," *J. Electrochem. Soc.*, **151** [10] B558–62 (2004).

[13]E. J. Opila, S. R. Levine, and J. Lorincz, "Oxidation of ZrB_2- and HfB_2 Based Ultra-High Temperature Ceramics: Effect of Ta Additions," *J. Mater. Sci.*, **39**, 5969–77 (2004).

Fig. 7. Backscattering electron microscopy (BSE) image of the silica (SiO_2) outermost layer containing zirconia (ZrO_2) particulate peaks.

[14]F. Monteverde, A. Bellosi, and S. Guicciardi, "Processing and Properties of Zirconium Diboride-Based Composites," *J. Eur. Ceram. Soc.*, **22**, 279–88 (2002).

[15]F. Monteverde, S. Guicciardi, and A. Bellosi, "Advances in Microstructure and Mechanical Properties of Zirconium Diboride Based Ceramics," *Mater. Sci. Eng.*, **A346**, 310–9 (2003).

[16]F. Monteverde and A. Bellosi, "Oxidation of ZrB_2-Based Ceramics in Dry Air," *J. Electrochem. Soc.*, **150** [11] B552–9 (2003).

[17]F. Monteverde and A. Bellosi, "The Resistance to Oxidation of HfB_2–SiC Composite," *J. Eur. Ceram. Soc.*, **25**, 1025–31 (2005).

[18]F. Monteverde, "The Thermal Stability in Air of Hot Pressed Diboride Matrix Composites for Uses at Ultra-High Temperatures," *Corrosion Sci.*, **47**, 2020–33 (2005).

[19]L. Scatteia, R. Borelli, G. Marino, A. Bellosi, and F. Monteverde, "Characterization and Process of New Metal Diboride Compound for TPS Applications"; AIAA/CIRA 13th International Space Planes and Hypersonic Systems and Technology Proceedings. American Institute of Aeronautics and Astronautics, Reston, VA, 2005.

[20]F. Monteverde and A. Bellosi, "Development and Characterization of Metal-Diboride-Based Composites Toughened with Ultra-Fine SiC Particulates," *Solid State Sci.*, **7** [5] 622–30 (2005).

[21]A. Chamberlain, W. Fahrenholtz, G. Hilmas, and D. Ellerby, "Oxidation of ZrB_2–SiC Ceramics under Atmospheric and Reentry Conditions," *Refractories Appl. Trans.*, **1** [2] 1–8 (2005).

[22]W. G. Fahrenholtz, "The ZrB_2 Volatility Diagram," *J. Am. Ceram. Soc.*, **88** [12] 3509–12 (2005).

[23]M. M. Opeka, I. G. Talmy, E. J. Wuchina, J. A. Zaykoski, and S. J. Causey, "Mechanical, Thermal, and Oxidation Properties of Refractory Hafnium and Zirconium Compounds," *J. Eur. Ceram. Soc.*, **19**, 2405–14 (1999).

[24]C. R. Wang, J. M. Yang, and W. Hoffmann, "Thermal Stability of Refractory Carbide/Boride Composites," *Mater. Chem. Phys.*, **74**, 272–81 (2002).

[25]M. Gasch, D. Ellerby, E. Irby, S. Beckman, M. Gusman, and S. Johnson, "Processing, Properties and Arc Jet Oxidation of Hafnium Diboride/Silicon Carbide Ultra High Temperature Ceramics," *J. Mater. Sci.*, **39**, 5925–37 (2004).

[26]I. Terrazas-Salinas and C. Cornelison, "Test Planning Guide for ASF Facilities"; A029-9701-XM3 Rev. B Thermophysics Facilities Branch, Space Technology Division, NASA Ames Research Center, CA, March, 1999.

[27]A. L. Cabrera and J. F. Kirner, "A Rapid-Temperature-Cycling Apparatus for Oxidation Testing," *Oxidation Metals*, **35** [5/6] 471–9 (1991).

[28]S. N. Karlsdottir, J. W. Halloran, F. Monteverde, and A. Bellosi, "Oxidation of ZrB2–SiC: Comparison of Furnace Heated Coupons and Self-Heated Ribbon Specimens (in press).

[29]N. S. Jacobson, "Corrosion of Silicon-Based Ceramics in Combustion Environments," *J. Am. Ceram. Soc.*, **76** [1] 3–28 (1993).

[30]S. N. Karlsdottir, J. W. Halloran, and A. N. Grundy, "Zirconia Transport by Liquid Convection during Oxidation of Zirconium Diboride-Silicon Carbide," *J. Am. Ceram. Soc.*, (in press; 2007). ☐